

MEHODS – DETAILS

Definition of QM and MM regions in QM/MM ONIOM calculations

In the case of S1 and S2 QM part consisted of E316, Y318, H450, E451, H455, E508 and H568 side chains, two zinc ions and six water molecules (see Fig. S1 c), while in the case of S3, E316, H450, E451, H455 and E508 side chains, two zinc ions and seven water molecules were considered as part of the QM layer (Fig. S1 d). In the structure of the complex besides E316, Y318, H450, E451, H455, E508 and H568 side chains, two zinc ions and five water molecules, peptide IVYPW main chain atoms (for proline the whole residue) were also considered as a part of QM layer (Fig. S1 e). The MM part (the rest of the protein) was treated using the AMBER force field (parm96).¹ To take into account solvation, water molecules from the enzyme first and second solvation sphere (additional 3229, 3523 and 3362 water molecules in the case of the S1 (and S2), S3 and CPLX1 (and CPLX2), respectively) were considered as a part of the MM layer as well.

MD simulations details

System minimization was performed in 4 cycles, followed heating, density equilibration and productive MD simulations. In the first cycle of optimization (1500 steps), water molecules were relaxed, while the rest of the system was harmonically restrained with a force constant of 64 kcal/(mol Å²). In the second cycle (2500 steps), a force constant (12 kcal/(mol Å²)) was applied to the zinc ion and the protein backbone, while the residues coordinated to the zinc ions and E451 were constrained with 64 kcal/(mol Å²). In the third cycle (1500 steps), a force constant to the zinc ion and the protein backbone was reduced to 6 kcal/(mol Å²), while force on the selected residues was reduced to 12 kcal/(mol Å²). In the final stage of minimization (1500 step) only the catalytic zinc ion, ZnA, and its coordinating residues were constrained (zinc with 6 kcal/(mol Å²) and its ligands with 12 kcal/(mol Å²)). Minimizations were performed using 470 steps of steepest descent followed by the conjugated gradient for the remaining steps.

The energy optimized system was heated from 0 to 300 K and equilibrated in 5 stages. In the first stage, system was heated from 0 K to 300 K during 10 ps using NVT ensemble with an integration step of 1 fs. During this stage protein backbone was constrained with 22 kcal/(mol Å²), zinc ions were constrained with 12 kcal/(mol Å²) and the inhibitory zinc ion (ZnI)

coordinating residues with 12 kcal/(mol Å²). This was followed by 70 ps of NPT ensemble simulations where constrains of 12 kcal/(mol Å²) were imposed only to the amino acid residues coordinating metal ions and metal ions itself. Followed 120 ps of MD simulations with constrains reduced to 6 kcal/(mol Å²). In the fourth stage (100 ps) only zinc ions were constrained with 6 kcal/(mol Å²), while in the final 700 ps of equilibration all constrains were released. The SHAKE algorithm was used to constrain covalent bonds involving hydrogens. The pressure was maintained with Berendsen barostat¹ at 1 atm with the pressure relaxation time of 1 ps, while the system temperature was held constant at 300 K using the Langevin thermostat² with a collision frequency of 5 and 2 ps⁻¹ (for the first three and the last two equilibration steps, respectively). Simulations were performed using periodic boundary conditions (PBC) with a cutoff value of 11 Å while the particle mesh Ewald (PME) method was used for calculation of the long-range electrostatic interactions.

Productive MD simulations were performed with time step of 1 and 2 fs (in the case of utilizing dummy atoms model and the 12-6 model for the zinc ions, respectively). In MD simulations performed utilizing 6-12 model **2** and dummy atom model **D2** charge on E451 was reduced to -0.75e and -0.65, respectively.

ASMD simulations

We performed ASMD simulations in which we simulated a) entrance of zinc ion to the enzyme, b) exit of the metal ion (ZnI) from the inhibitory metal binding site and its translocation to the protein surface. In both cases the active metal binding site (defined with H450, H455 and E508) was occupied with zinc ion (ZnA). In simulations of the metal ion exit, the distance between the protein surface and the exiting entity was defined as the distance between Zn and the carboxyl groups of the residues D396 and D496 center of mass. The distance was gently decreased from 12.0 - 2.0 Å using a force constant of 7.2 kcal mol⁻¹Å⁻² and velocity of 1 Å/ns. Simulations were carried out in five, 2 ns long stages, with 25 replicas performed for each stage. In simulations of zinc ion entering the enzyme, initial structure of ZnI was completely solvated (coordinated with 6 water molecules). ASMD simulations were carried out in twelve, 2 ns long stages, with 25 replicas performed for each one. After each step, the structure closest to the Jarzynski² average was determined and used as the starting point for the next step. For ASMD simulations, the NVT ensemble was used. Time step in simulations was 1 fs.

Table S1 Metal ion models used within this work.

Model	#	charge/e				E451
		Zn				
Dummy atom	D1 ¹	Total	central point (carry vdw parameters)	δ points at z- axis of octahedron	points at x and y axes of octahedron	
		D2 ²	2	-1	0.5	
		1.325	-0.475	0.1	0.4	
6-12	1 ³	2.0				-0.75
	2	1.375				
	3	ZnA 1.1, ZnI 0.9				
	3'	1.0				
	3r	ZnA 0.9, ZnI 1.1				

¹ F. Duarte, P. Bauer, A. Barrozo, B. A. Amrein, M. Purg, J. Åqvist and S. C. L. Kamerlin, *J. Phys. Chem. B*, 2014, **118**, 4351–4362.

² The barrier for angles involving at least one of the dummy atoms was set to 0 in this model to allow plasticity of the coordination sphere.

³ A. Tomić, M. Berynsky, R. C. Wade and S. Tomić, *Mol. Biosyst.*, 2015, **11**, 3068–3080.

Table S2 MD simulations of several DPP III structures with 2 zinc ions bound into the substrate binding site and solvated in water Na⁺ solution (Na⁺ ions are added for the purpose of system neutralization). Given are the data for the structures (metal ion coordination) that were the most populated during particular MD simulation. Time period (in μs) the particular metal ion coordination was present (t_i) and the total simulation time (t_{total}) are given in third column. The metal ligands present in the initial structures are given in bold. MMGBSA energies calculated at the trajectory sections where the metal ion coordination corresponds to the most populated coordination determined during particular simulation.

a) Simulations performed using 6-12 models (1-3) for the zinc ions. See Table S1 for models definition.

Model #	SIMULATED SYSTEM Force field	t_i/t_{total}^a ($\mu\text{s}/\mu\text{s}$)	$\langle \text{ZnA} - \text{ZnI} \rangle$ (\AA)	ZnA ligands (coordinated with)	ZnI ligands (coordinated with)	MMGBSA(kcal/mol) ^b		
						Receptor: DPP III Ligand: Zn _A + Zn _I	Receptor: DPP III + ZnA Ligand: Zn _I	Receptor: DPP III Ligand: ZnA
1	S1 ff03	0.2/0.2	4.7 \pm 0.2	H450, H455, E508^M, E451^M mostly 4 W	E508^M, H568, E316^B mostly 3 W	-20 \pm 5	6 \pm 3	-21 \pm 3
	S1 ff03	0.6/0.6	5.5 \pm 0.2	H450, H455, E508^M, E451^M mostly 2 W	E508^M, E316^M , mostly 4 W	2 \pm 5	26 \pm 3	-19 \pm 4
	S1 ff14SB	0.3/0.3 ^{ZnA} 0.15/0.3 ^{ZnI}	4.9 \pm 0.1	H450, H455, E508^M, E451^{B,M} mostly 2 W	E508^M, E316^M , mostly 4 W	24 \pm 4	28 \pm 3	2 \pm 2
2	S2 ff03	0.85/1	4.0 \pm 0.4	H450, H455, E508^M, E451^M W 1-4	E508^B, E316^B W 1-4	-31 \pm 4	-2 \pm 2	-27 \pm 3
	S1 ff03	0.99/1 ^{ZnA} 0.81/1 ^{ZnI}	3.8 \pm 0.2	H450, H455, E508^M, E451^M mostly 2 W	E508^M, E316^B mostly 3 W	-32 \pm 4	1 \pm 3	-26 \pm 3
	S2 ff03	0.42/0.45 ^{ZnA} 0.24/0.45 ^{ZnI} 0.12/0.45 ^{ZnI}	3.9 \pm 0.2	H450, H455, E508^M, E451^{M**} mostly 1 W	E508^M, E316^B , mostly 3 W	-25 \pm 5	3 \pm 2	-26 \pm 2
					E316^B mostly 3 W	-20 \pm 5	10 \pm 3	-26 \pm 1

	S1-OH⁻ ff03	0.25/0.35 ^{ZnA} 0.21/0.35 ^{ZnI}	3.5 _± 0.3	H450, H455, E508^M, E451^M, OH⁻	E316 ^B E508 ^B , OH ⁻ mostly 3 W	-24 _± 6	13 _± 5	-27 _± 4
	CPLX1 ff03	0.24/0.25 ^{ZnA} 0.24/0.25 ^{ZnI}	5.2 _± 0.3	H450, H455, E508^M, E451 ^M 1-2 W	H565, E508^M mostly 2 W	-26 _± 2	0 _± 1	-22 _± 2
3	S1-OH⁻ * ff03	0.40/0.44 ^{ZnA} 0.17/0.44 ^{ZnI}	7.0 _± 3.2	H450, H455, E508^{B,M}, OH⁻ 0-1 W	E316 ^{B,M} , 2-3 W	-52 _± 5	-4 _± 3	-43 _± 3
	S1 -OH⁻ * ff03	0.18/0.2 ^{ZnA} 0.11/0.2 ^{ZnI}	4.8 _± 2.5	H450, H455, E508^M, OH⁻ mostly 1 W	E508^M, H568, OH⁻ 1-3 W	-83 _± 5	-26 _± 3	-51 _± 3
	S1- OH⁻ * ff14SB	0.34/0.35 ^{ZnA} 0.16(0.11)/0.35 ^{ZnI}	6.0 _± 0.8 3.5 _± 0.2 (last 110 ns)	H450, H455, E508^{B,M}, OH⁻ mostly 1 W	E316 ^M , H568, (E316 ^M , E451, OH ⁻) ^d 1-3 W	-46 _± 6	-6 _± 4	-36 _± 4
	S1- OH⁻ * ff14SB	0.69/0.7 ^{ZnA} 0.55/0.7 ^{ZnI}	3.5 _± 0.2 (last 590 ns)	H450, H455, E508^M, OH⁻ 1-2 W	E451 ^{M,B} , OH⁻ 2-3 W	-49 _± 4	-11 _± 4	-35 _± 3
	S1- OH⁻ *exc ff14SB	0.5/1.0 ^{ZnA} 0.87/1.0 ^{ZnI}	10.0 _± 0.7 (last 740 ns)	N294, E316 ^M mostly 2-3 W	H450, H455, E508^M mostly 1-2 W	-27 _± 4	-14 _± 4	-12 _± 2
	CPLX1 ff14SB	1.1/1.1 ^{ZnA} 1.1/1.1 ^{ZnI}	4.0 _± 0.2	H450, E451^{M,B} H455, E508^M, 1 W	H568, E508^{M,B} ^c HM-O2nd mostly 1 W	-34 _± 4	-1 _± 3	-23 _± 3
	CPLX1 ff14SB	1.1/1.2 ^{ZnA} 0.5/1.2 ^{ZnI}	4.0 _± 0.2	H450, E451^{B,M} H455, E508^M, 1 W	H568, E508^M ^c HM-O2nd 1 W	-31 _± 3	-2 _± 2	-22 _± 3
	CPLX2 ff14SB	0.32/0.34 ^{ZnA} 0.32/0.34 ^{ZnI}	11.6 _± 0.9	H450, H455, E508^M, mostly 2 W	D396 ^{M,B} , D496 ^{M,B} 1-2 W	-25 _± 3	-12 _± 2	-12 _± 3
	CPLX2 ff14SB	0.28/0.28 ^{ZnA} 0.08/0.28 ^{ZnI}	18.6 _± 12.7	H450, H455, E508^M, 1 W	E508 ^M ^c HM-O2nd, 1 W	-21 _± 5	-4 _± 3	-17 _± 3
3'	CPLX2 ff14SB	0.94/1.0 ^{ZnA} 1.0/1.0 ^{ZnI}	3.8 _± 0.2	H450, H455, E508^{M,B} mostly 1 W	H568, E508^{M,B} ^c HM-O2nd mostly 2 W	-11 _± 4	4 _± 3	-8 _± 3
3r	CPLX2^{exc} ff14SB	0.44/0.98 ^{ZnA} 0.41/0.98 ^{ZnI}	4.5 _± 0.4	H450, H455, E451^{M,B} mostly 1W	H450, H455, , E508 ^{M,B} ^c HM-O2nd mostly 1 W	-23 _± 2	-2 _± 1	-21 _± 2

^aTime period the most populated system is present

^bMMGBSA energies calculated at the regions of trajectory with the most representative (populated) structure regarding the zinc ions coordination.

^cDuring this MD simulation exchange of zinc ions occurred, see Fig. S6.

^dOH⁻ coordinate ZnI during the last 110 ns of MD simulation.

OH⁻ bridges two zinc ions, ZnA and ZnI

*OH⁻ is H-bonded to the carboxyl (COOH) group of Glu451

b) Simulations performed using dummy atom models (**D1-D2**) for the zinc ions. See Table S1 for models definition.

Model #	SYSTEM Force field	t _i /t _{total} (μs)	<ZnA–ZnI> (Å)	ZnA ligands	ZnI ligands	MMGBSA(kcal/mol)		
						Receptor: DPP III Ligand: ZnA + ZnI	Receptor: DPP III Ligand: ZnA	Rec: DPP III+ ZnA Ligand: ZnI
D1	S1 ff14SB	0.099/0.1 ^{ZnA} 0.095/0.1 ^{ZnI}	5.4±0.1 51%	H450, H455, E508^M, E451^M 2W	H568, E316^B, E508^M, Y315 2W	-292±11	-164±6	-108±7
	S1 ff03	0.1/0.1	5.4±0.1 51% 5.1±0.1 49%	H450, H455, E508^M, E451^M 2W	E316 ^M , E508^M, H568 3W	-320±8	-187±6	-121±6
D2	S1 ff03	0.085/0.1 ^{ZnA} /0.1/0.1 ^{ZnI}	3.5±0.2	E508^M, H450, H455 mostly 3W	E316 ^M , E508^M mostly 3W	-144±6	-80±5	-47±7
	S1 ff03	0.066/0.1 ^{ZnA} 0.056/0.1 ^{ZnI}	4.9±0.5	E508^M, H450, H455 3W	E316 ^M , E508^M, H568 3W	-166±8	-81±5	-50±10
	S1 ff14SB	0.58/1 ^{ZnA} 0.88/1 ^{ZnI}	5.4±0.3	H450, H455, E508^M 3-4W	E316 ^M , E508^M mostly 4 W	-122±8	-67±5	-48±7
	S2 ff14SB	0.5/1 ^{ZnA} 0.99/1 ^{ZnI}	4.7±0.5	H450, H455, E508^M 3-4W	E316^M, E508^M 4-5W	-116±7	-68±5	-43±5
	S1 ff14SB	0.062/0.1 ^{ZnA} 0.1/0.1 ^{ZnI}	4.1±0.3	H450, H455, E508^M 3W	E508^M 4-5 W	-102±9	-69±4	-23±6
	S1 ff14SB	0.22/0.25 ^{ZnA} 0.16/0.25 ^{ZnI}	4.7±0.1	H450, H455, E508^M, E451^M	H568, E508^M, V730 2-3W	-160±7	-96±5	-57±5

				1W				
	CPLX1 ff14SB	0.5/0.5 ^{ZnA} 0.5/0.5 ^{ZnI}	5.2±0.3	H450, H455, E508^{M,B},E451 mostly 1 W	E508^M mostly 4 W	-114±7	-93±5	-18±4
	CPLX2 ff14SB	0.5/0.5 ^{ZnA} 0.44/0.5 ^{ZnI}	5.4±0.3	H450, H455, E508^{M,B} 1W	H568, E508^{M,B} ^cHM-O2nd mostly 2 W	-150±8	-85±5	-39±4

Table S3. Selected distances in the two zinc ions hDPP III structures before (I) and after QM/MM optimization at B97D/[6-31(G)d + LanL2DZ-ECP] level of theory with charge embedding.

	<i>d</i> / Å							
	I ^a	S1	S2	I	S3	I ^b	CPLX1	CPLX2
ZnA-ZnI	3.45	3.78	4.31	5.05	4.95	5.30	4.75	5.54
ZnA-H450(ne2)	2.34	2.11	2.14	2.29	2.19	2.19	2.11	2.15
ZnA-E451(oe1)	3.82	3.76	3.89	4.43	4.10	4.12 / 3.67	4.03	3.48
ZnA-E451(oe2)	3.98	4.66	4.47	4.84	4.72	2.93 / 2.19	3.67	2.18
ZnA-H455(ne2)	2.45	2.10	2.21	2.39	2.16	2.29	2.14	2.17
ZnA-E508(oe2)	2.18	2.03	2.06	2.05	2.14	2.17	2.02	2.10
ZnA-W1(ow)	2.20	2.00	2.03	2.14	2.14	2.19	1.95	2.13
ZnA-W2(ow)	2.31	3.01	3.45	2.51	2.26	6.08	5.50	5.50
ZnA-W3(ow)	2.49	2.98	2.82	2.16	2.32	5.75	5.00	5.65
ZnA-W4(ow)	4.58	4.73	5.99	6.06	4.62	7.07	6.26	5.78
ZnA-W5(ow)	4.08	4.45	2.39	7.02	6.87	9.71	8.72	8.31
ZnA-W6(ow)	4.44	3.94	5.65	6.29	6.19			
ZnA-W7(ow)				6.13	6.18			
ZnI-E508(oe1)	2.17	2.16	3.98	2.06	2.09	2.20	2.29	4.26
ZnI-H568(ne2)	2.35	2.20	2.18	9.59	9.57	2.30	2.23	2.19
ZnI-Y318(oh)	2.53 / 4.19	2.22	4.79	9.28	9.98	2.60	2.28	2.17
ZnI-E316(oe1)	4.16 / 3.88	3.81	3.21	3.72	3.87	3.88	3.84	4.06
ZnI-E316(oe2)	3.89 / 2.75	4.03	2.10	2.07	2.11	5.66	5.97	6.18
ZnI-W1(ow)	4.42	3.84	4.28	6.49	6.08	4.90	4.88	4.71
ZnI-W2(ow)	2.49	2.13	2.16	5.44	5.80	3.77	3.67	4.00
ZnI-W3(ow)	2.46	2.21	2.17	3.76	3.44	2.30	2.15	2.21
ZnI-W4(ow)	2.21	2.14	2.16	2.93	2.22	2.30	2.20	2.17
ZnI-W5(ow)	5.63	5.22	4.22	2.14	2.15	4.60	4.40	3.66
ZnI-W6(ow)	5.25	4.77	3.35	2.11	2.21			
ZnI-W7(ow)				2.45	2.15			
W1(ow)-W1(hw1)	0.96	0.99	0.98	0.98	0.99	0.96	0.97	0.97
W1(ow)-W1(hw2)	0.96	1.53	1.51	0.99	1.05	0.96	1.38	1.03
W2(ow)-W2(hw1)	0.96	0.99	0.99	0.98	1.00	0.96	0.98	1.00
W2(ow)-W2(hw2)	0.96	1.03	1.00	0.99	1.00	0.96	0.99	0.99
W3(ow)-W3(hw1)	0.96	0.97	1.01	0.99	1.00	0.96	0.99	1.00
W3(ow)-W3(hw2)	0.96	1.02	1.00	0.99	1.00	0.96	1.00	0.98
W4(ow)-W4(hw1)	0.96	0.97	0.98	0.98	0.97	0.96	1.00	1.00
W4(ow)-W4(hw2)	0.96	1.02	1.02	0.99	1.00	0.96	1.00	1.00
W5(ow)-W5(hw1)	0.96	0.98	1.01	0.98	0.99	0.96	0.98	1.01
W5(ow)-W5(hw2)	0.96	0.99	0.98	0.99	1.00	0.96	0.99	0.98
W6(ow)-W6(hw1)	0.96	0.97	1.01	0.99	0.99			
W6(ow)-W6(hw2)	0.96	0.98	0.98	0.99	0.99			
W7(ow)-W7(hw1)				0.98	0.99			
W7(ow)-W7(hw2)				0.98	1.02			

E451(oe1)-W1(hw2)	1.51	1.06	1.08	1.67	1.52	1.74 / 2.15	1.11	1.61
E316(oe2)-W3(hw1)	3.14 / 3.62	3.01	3.49	1.64	1.82	4.63	4.93	5.64
E316(oe2)-W3(hw2)	1.73 / 2.78	1.65	2.69	2.88	3.31	3.57	3.64	4.77
E316(oe1)-W3(hw2)	3.43 / 2.61	2.95	1.75	4.41	4.86	1.84	1.72	2.90
E316(oe1)-W4(hw2)	1.69 / 1.95	1.61	3.57	4.65	4.83	4.17	5.01	5.60
E316(oe2)-W4(hw2)	2.53 / 2.58	2.67	2.94	3.50	2.95	6.83	7.11	7.42
E316(oe2)-W6(hw2)	1.83 / 4.28	2.00	2.85	4.89	4.80			
E316(oe1)-W6(hw2)	3.48 / 2.85	3.75	1.94	6.24	6.10			
Y318(hh)-E508(oe1)	3.97 / 1.66	4.15	1.79	10.08	10.70	5.17	4.94	6.25
Y318(hh)-E316(oe1)	2.28 / 5.69	1.62	5.41	11.80	12.37	1.85	1.72	1.74
Y318(hh)-E316(oe2)	2.16 / 3.64	2.83	4.65	10.27	11.21	3.59	3.84	4.00
E508(oe1)-W3(hw1)	3.54	2.55	1.67	2.63	2.69	3.56	3.44	3.14
E508(oe1)-W2(hw1)	4.56	3.84	4.80	3.90	4.42	2.12	1.83	1.16
ZnI-O _{supst}						2.35	2.14	2.06

^a Values in **S2** that differ from those in **S1** and (right and left, respectively).

^b Values in **CPLX2** that differ from those in **CPLX1** (right and left, respectively).

Table S4. Energies (and their differences) computed with the ONIOM methodology utilizing the B97D/[6-31(G)d + LanL2DZ-ECP] level of theory for the QM layer, and Amber parm96 force field for the MM layer. $E^{MM}(M)$ and $E^{MM}(R)$ give the energies of the model (M) and real (R) system, respectively, at the low accuracy method, wherein $E^{QM}(M)$ energy of the model system at the high accuracy method. E^{ONIOM} is the ONIOM total energy.

	S1	S2	$\Delta = S1 - S2$	
$E^{MM}(M)/\text{kcal mol}^{-1}$	-1469.96	-1501.38	$\Delta E^{MM}(M)/\text{kcal mol}^{-1}$	31.42
$E^{QM}(M)/\text{kcal mol}^{-1}$	-1590755.14	-1590770.24	$\Delta E^{QM}(M)/\text{kcal mol}^{-1}$	15.10
$E^{MM}(R)/\text{kcal mol}^{-1}$	-39106.50	-39117.72	$\Delta E^{MM}(R)/\text{kcal mol}^{-1}$	11.21
$E^{ONIOM}/\text{kcal mol}^{-1}$	-1628391.68	-1628386.57	$\Delta E^{ONIOM}/\text{kcal mol}^{-1}$	-5.10

	CPLX2	CPLX1	$\Delta = CPLX2 - CPLX1$	
$E^{MM}(M)/\text{kcal mol}^{-1}$	-940.47	-1751.72	$\Delta E^{MM}(M)/\text{kcal mol}^{-1}$	811.25
$E^{QM}(M)/\text{kcal mol}^{-1}$	-2315821.57	-2315809.38	$\Delta E^{QM}(M)/\text{kcal mol}^{-1}$	-12.19
$E^{MM}(R)/\text{kcal mol}^{-1}$	-45642.95	-46461.53	$\Delta E^{MM}(R)/\text{kcal mol}^{-1}$	818.58
$E^{ONIOM}/\text{kcal mol}^{-1}$	-2360524.06	-2360519.19	$\Delta E^{ONIOM}/\text{kcal mol}^{-1}$	-4.87

Table S5. The ONIOM calculated ESP charges for the whole system. Values for atoms described quantum mechanically (utilizing B97D/[6-31(G)d + LanL2DZ-ECP] level of theory) are shown.

Residue	Atom name	S1	S2	S3	CPLX1	CPLX2
GLU316	CB	-0.089324	-0.319739	-0.356837	-0.084928	-0.276494
	HB2	0.051013	0.141189	0.170904	0.06153	0.092067
	HB3	-0.052636	0.056291	0.0942	-0.048237	0.017205
	CG	-0.088354	0.033603	-0.243881	0.151137	0.04336
	HG2	0.058097	-0.029791	0.127118	-0.05155	0.028105
	HG3	0.096648	0.048043	0.053713	0.021612	0.107271
	CD	0.796657	0.575377	0.909565	0.407101	0.72433
	OE1	-0.746874	-0.610213	-0.715857	-0.350946	-0.666406
OE2	-0.816321	-0.736914	-0.828443	-0.507134	-0.626042	
TYR318	CB	-0.457941	-0.495233		-0.542032	-0.498795
	HB2	0.123531	0.078519		0.13695	0.124501
	HB3	0.150727	0.120255		0.179444	0.159853
	CG	0.314097	0.316231		0.389872	0.311393
	CD1	-0.315952	-0.260862		-0.34904	-0.279417
	HD1	0.131175	0.195937		0.199507	0.193563
	CE1	-0.162579	-0.297344		-0.14937	-0.290376
	HE1	0.141133	0.146225		0.148572	0.17038
	CZ	0.343333	0.34808		0.163718	0.42025
	OH	-0.563301	-0.531835		-0.50512	-0.918107
	HH	0.392761	0.400101		0.339318	0.635347
	CE2	-0.219203	-0.194326		0.002572	-0.268818
	HE2	0.160443	0.162684		0.112968	0.223598
	CD2	-0.27044	-0.25763		-0.360004	-0.230213
HD2	0.174209	0.170547		0.191287	0.190114	
HIS450	CB	-0.514015	-0.468016	-0.41179	-0.481699	-0.543635
	HB2	0.163518	0.147899	0.147828	0.162868	0.17022
	HB3	0.210919	0.188994	0.168328	0.207368	0.219173
	CG	0.288391	0.235654	0.158424	0.215837	0.263386
	ND1	-0.396507	-0.351896	-0.310322	-0.30108	-0.337893
	HD1	0.412158	0.401566	0.407667	0.401841	0.399141
	CE1	0.106853	-0.029472	-0.104209	-0.006389	0.055121
	HE1	0.120806	0.152191	0.179697	0.158863	0.135279
	NE2	-0.432842	-0.229321	-0.048421	-0.366471	-0.421624
	CD2	-0.0976	-0.156587	-0.253141	-0.084849	-0.145832
	HD2	0.121801	0.143784	0.192987	0.10541	0.149145
GLU451	CB	-0.233611	-0.226654	-0.263703	-0.404965	-0.237702
	HB2	0.037555	0.036317	0.029385	0.097112	0.066546
	HB3	0.071905	0.0682	0.068078	0.037843	0.018227
	CG	0.108275	0.10914	0.095378	0.254405	0.215569
	HG2	0.039213	0.032525	0.026147	-0.000618	-0.009051
	HG3	0.017815	0.011702	-0.005341	-0.006858	-0.029691
	CD	0.564646	0.579946	0.656158	0.552762	0.475114
	OE1	-0.627232	-0.633064	-0.725427	-0.550747	-0.607
	OE2	-0.613414	-0.617329	-0.759265	-0.727709	-0.626977
HIS455	CB	-0.503017	-0.517297	-0.567741	-0.572192	-0.536937
	HB2	0.09809	0.094023	0.120559	0.134701	0.116384
	HB3	0.142055	0.141898	0.142799	0.1187	0.111929
	CG	0.363079	0.367163	0.470112	0.386731	0.394455
	ND1	-0.311485	-0.343172	-0.404463	-0.363562	-0.349656
	HD1	0.464782	0.459786	0.451713	0.443659	0.444177

	CE1	-0.061085	0.034855	0.046135	0.095019	-0.005863
	HE1	0.226545	0.201946	0.197504	0.184143	0.206272
	NE2	-0.165	-0.329322	-0.187463	-0.441991	-0.236659
	CD2	-0.336429	-0.2656	-0.407627	-0.159707	-0.325632
	HD2	0.192963	0.156156	0.211211	0.132222	0.181353
GLU508	CB	-0.278155	-0.382354	-0.448574	-0.349516	-0.437205
	HB2	0.137386	0.18971	0.076381	0.110108	0.133188
	HB3	0.090833	0.077348	0.107207	0.105514	0.101645
	CG	-0.138522	-0.020983	0.178795	-0.095265	0.037058
	HG2	0.06281	0.057863	0.038547	0.075334	0.043597
	HG3	0.019426	-0.016786	-0.049621	0.037633	0.037763
	CD	0.709406	0.609435	0.706189	0.760854	0.512655
	OE1	-0.48752	-0.559177	-0.731322	-0.573563	-0.59368
	OE2	-0.711116	-0.677669	-0.637002	-0.775555	-0.75329
HIS568	CB	-0.487879	-0.517485		-0.567689	-0.538319
	HB2	0.15802	0.162711		0.146639	0.128699
	HB3	0.066565	0.053784		0.130885	0.123085
	CG	0.373622	0.450527		0.432752	0.565261
	ND1	-0.354259	-0.376904		-0.35777	-0.460842
	CE1	0.437554	0.425024		0.424967	0.442643
	HE1	0.072078	0.061734		0.0938	0.285675
	NE2	0.137978	0.157687		0.152933	0.133761
	HE2	-0.329362	-0.346467		-0.381635	-0.684271
	CD2	-0.251776	-0.317327		-0.171432	-0.365601
	HD2	0.156655	0.182142		0.14578	0.251342
ZnA	ZN	1.095133	1.02401	0.749966	1.182116	1.248365
ZnI	ZN	0.924497	1.261918	1.438083	0.972494	1.385655
W1	OW	-1.17679	-0.958692	-0.931077	-0.966258	-0.639536
	HW1	0.555335	0.387306	0.453937	0.345861	0.272928
	HW2	0.529035	0.486839	0.527032	0.585996	0.377933
W2	OW	-0.768324	-0.834378	-0.928566	-0.817555	-0.892788
	HW1	0.429888	0.407698	0.504281	0.350837	0.423411
	HW2	0.500071	0.455589	0.504825	0.499375	0.520663
W3	OW	-1.169939	-0.768216	-0.288718	-0.90326	-1.067916
	HW1	0.465216	0.352653	0.222901	0.294679	0.568029
	HW2	0.718983	0.392775	0.375829	0.594468	0.534906
W4	OW	-0.92793	-0.909529	-0.73809	-0.844866	-0.719297
	HW1	0.462212	0.454907	0.44151	0.410705	0.307598
	HW2	0.498468	0.485635	0.2157	0.452135	0.475159
W5	OW	-0.94199	-0.842886	-1.222386	-0.763622	-0.896901
	HW1	0.428234	0.488081	0.592998	0.330427	0.542104
	HW2	0.520065	0.463905	0.591531	0.477387	0.430207
W6	OW	-0.87123	-0.850895	-1.005956		
	HW1	0.38866	0.508176	0.5071		
	HW2	0.492829	0.39914	0.521825		
W7	OW			-0.913768		
	HW1			0.516631		
	HW2			0.504666		
Os					-0.412342	-0.407959

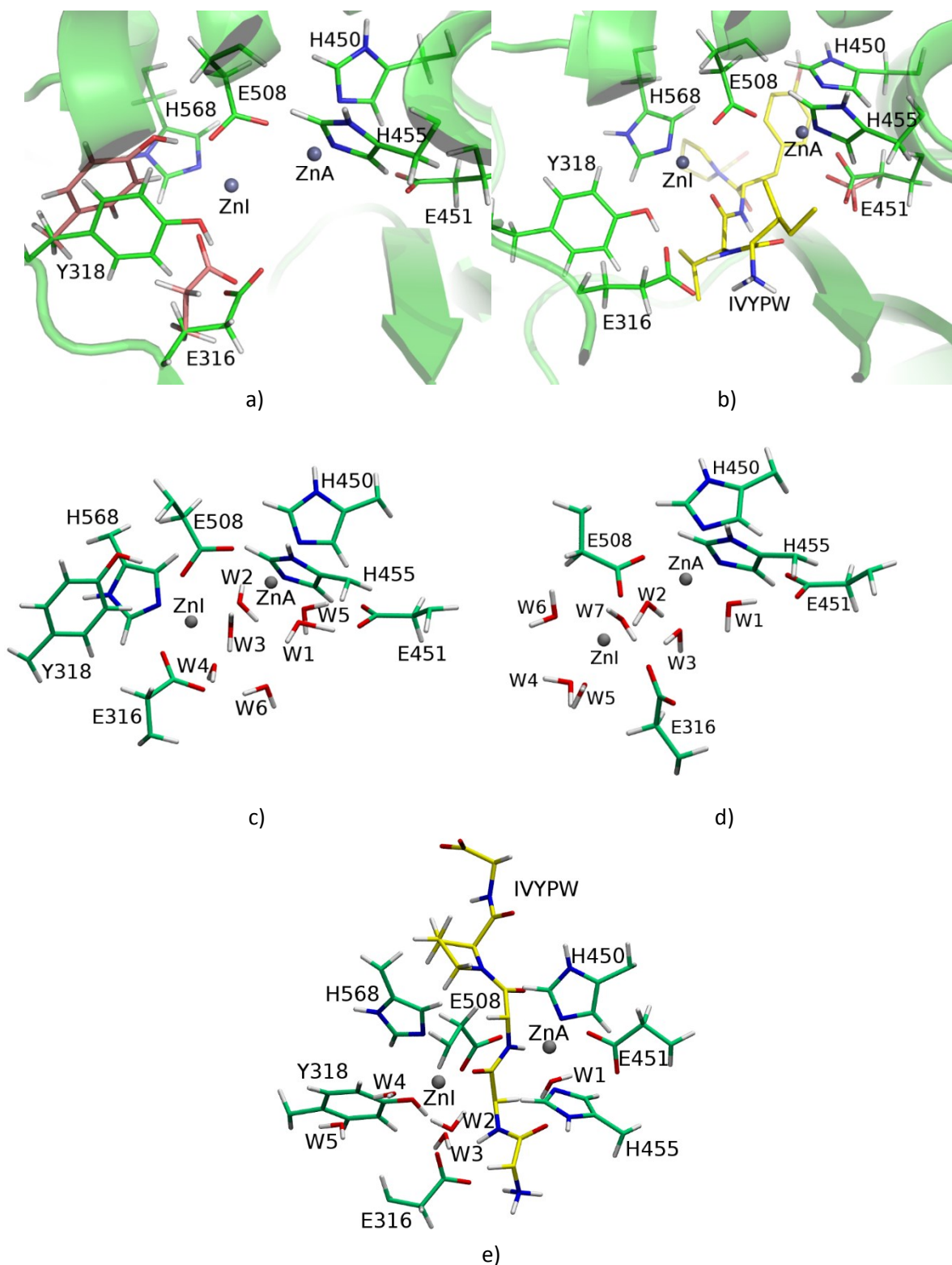


Figure S1. Active site geometries in: a) **S1** (green) and **S2** structures wherein the amino acid residues in **S2** with orientation different from those in **S1** are coloured pink, and b) in structure of the complexes **CPLX2** (green) and **CPLX1** wherein the amino acid residues in **CPLX1** with orientation different from those in **CPLX2** are shown in pink. Peptide IVYPW carbon atoms are coloured yellow (only polar hydrogens are shown) and solvent is not shown. In figures c), d) and e) the QM layers, as defined in the present QM/MM calculations, of **S1** (equally valid for **S2**), **S3**, and **CPLX1** (equally valid for **CPLX2**) are shown, respectively. Amino acid residues and water molecules are shown as sticks, and zinc ions as spheres. Link atoms are not shown.

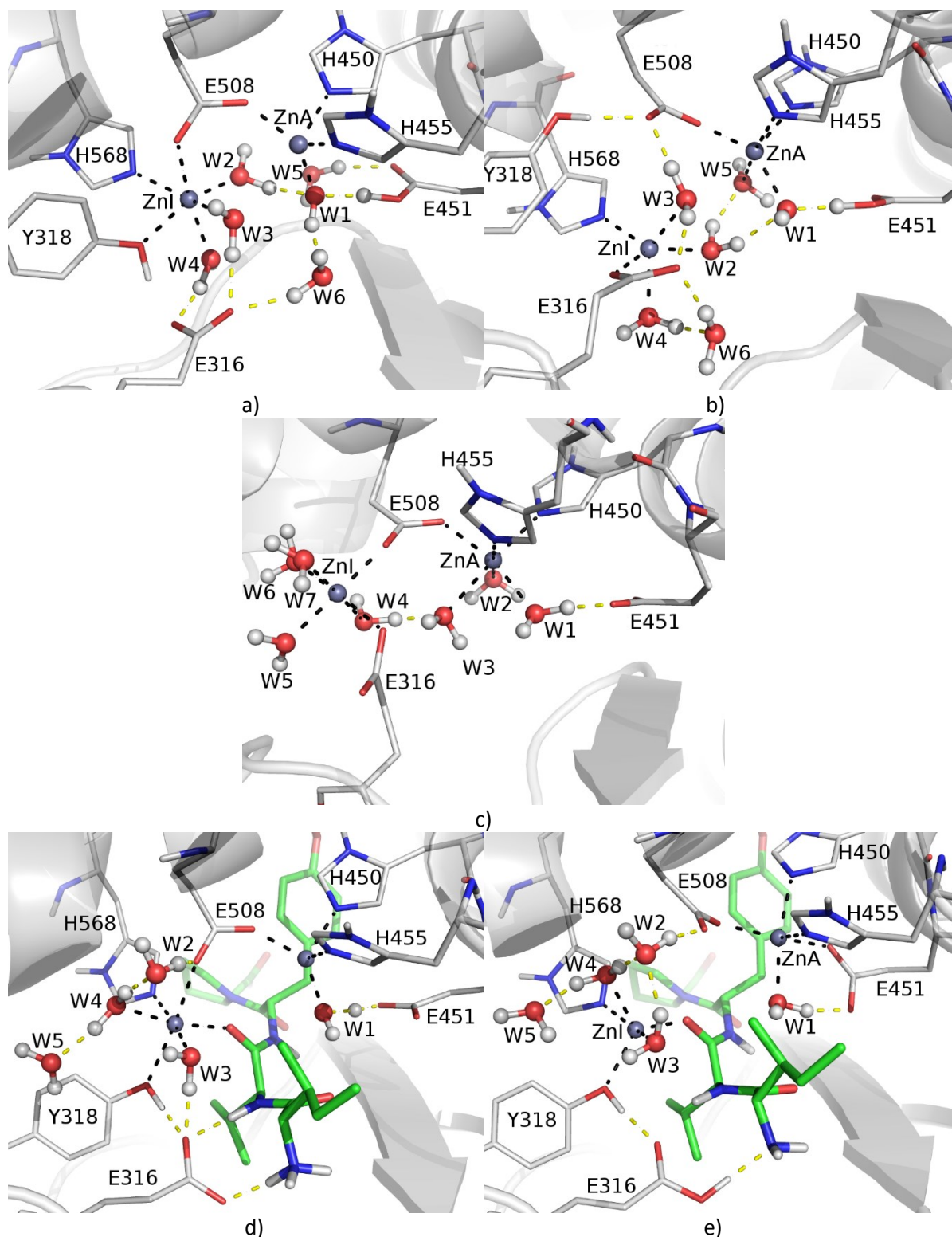


Figure S2. QM/MM optimized structures: a) S1, b) S2, c) S3, d) CPLX1 and e) CPLX2. Calculations were performed at the B97D/[6-31(G)d + LanL2DZ-ECP] level of theory for QM layer, and using Amber parm96 force field for MM layer. Residues represented as stick (amino acids), ball and stick (waters) and sphere (zinc ions) are treated at QM level of theory. Peptide IVYPW (stick representation) carbon atoms are colored green. Only polar hydrogens are shown. Coordinating bonds and some important hydrogen bonds are shown as black and yellow dashed lines, respectively. For distances see Tables 1 and S3.

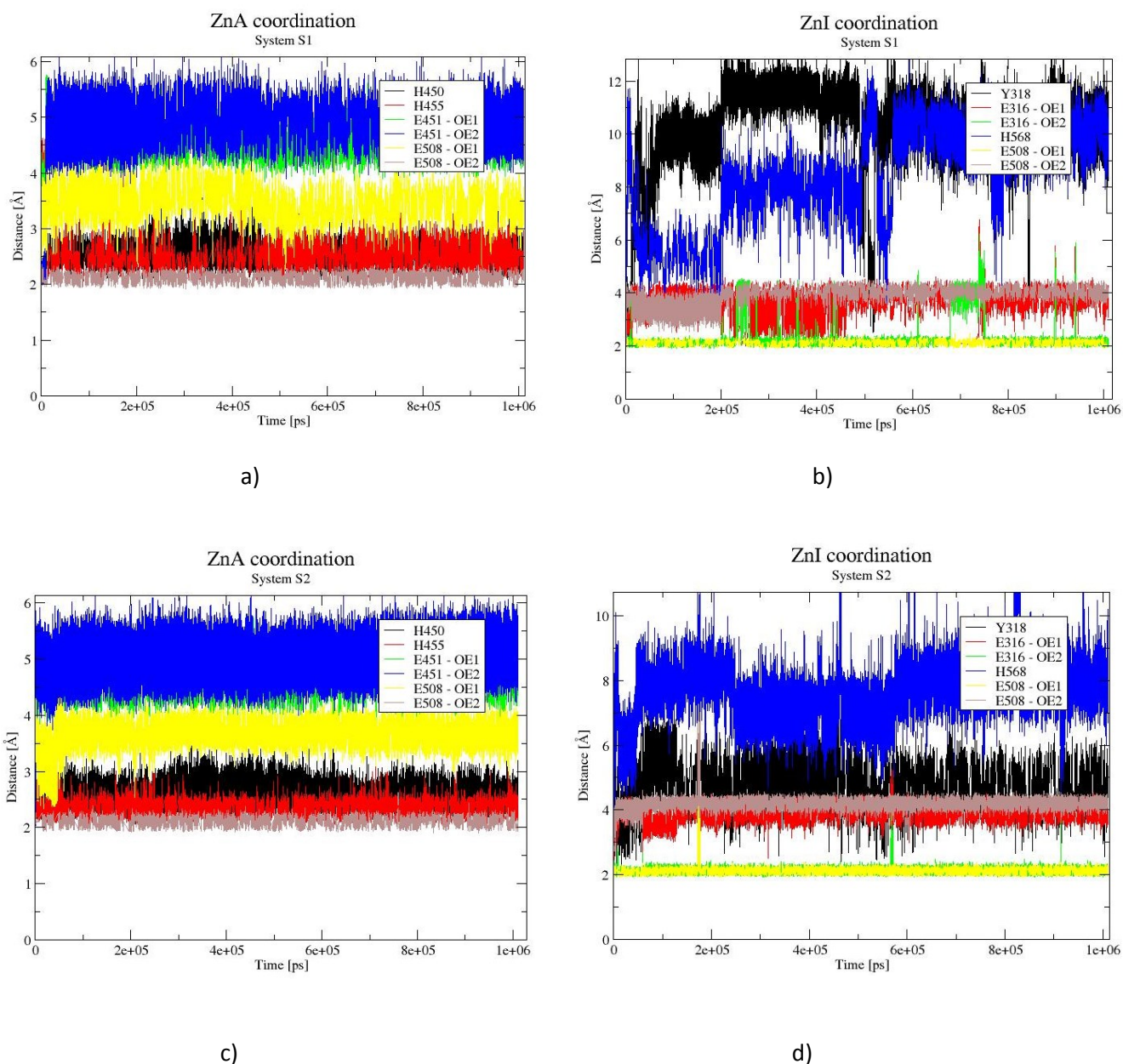


Figure S3. Coordination of zinc ions during 1 μs of MD simulations of structures S1 (a and b) and S2 (c and d) with model D2 and ff14SB force field: a) and c) distances from ZnA to Ne atoms of H450 and H455 (black and red, respectively), to carboxyl oxygens of E451 (blue and green), and to carboxyl oxygens of E508 (yellow and brown); b) and d) distances from ZnI to Y318 hydroxyl (black), to carboxyl oxygens of E316 (red and green), to Ne atom H568 (blue) and to carboxyl oxygens of E508 (yellow and brown).

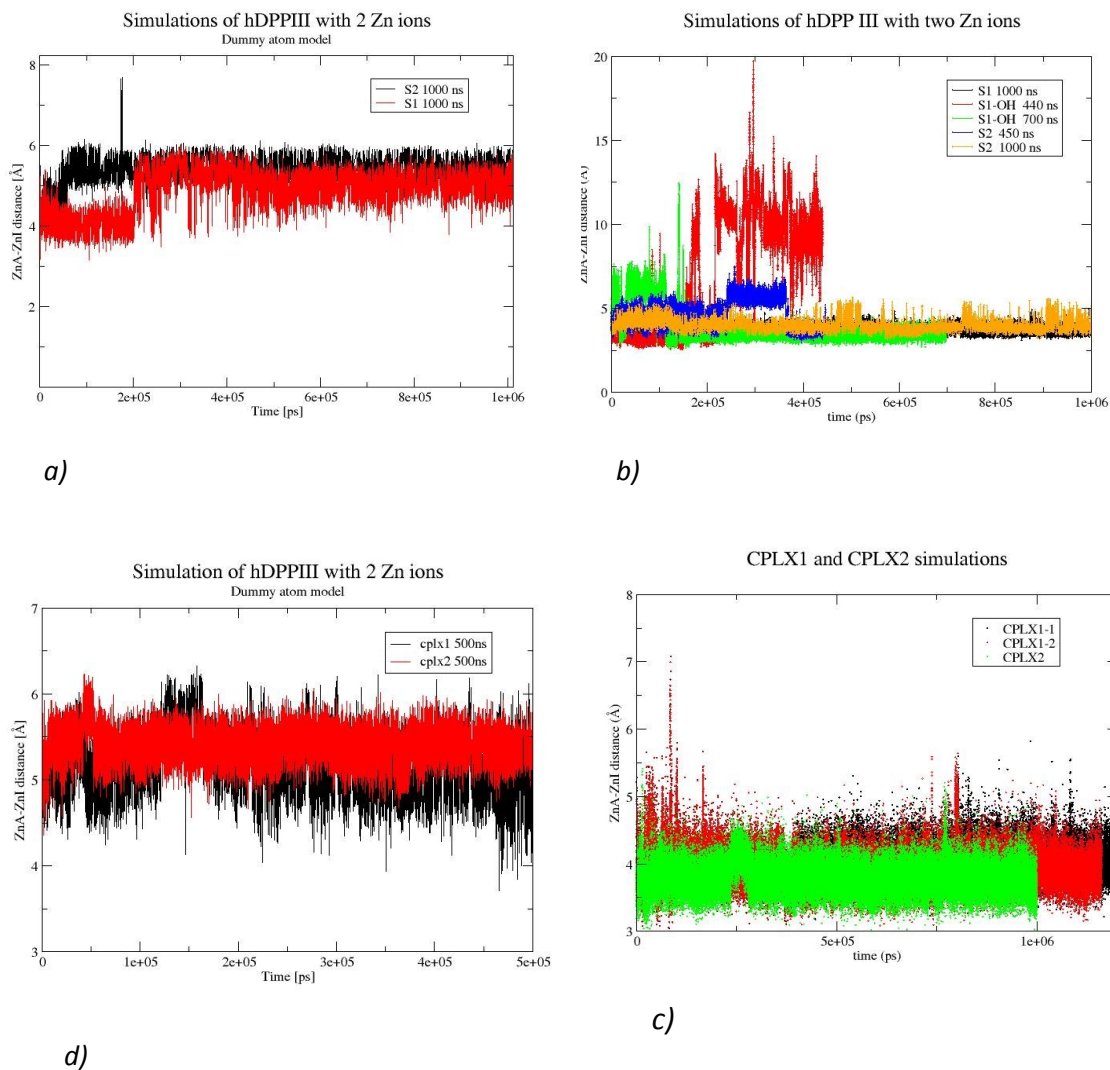


Figure S4. Distance between zinc ions during MD simulations longer of 350 ns: a) and b) distances the during simulations of the ligand free hDPP III with dummy atom model **D2** and 6-12 models, respectively; c) and d) distances during simulations of the hDPP III – IVYPW complex and with dummy atom model **D2** and 6-12 models. More parameters about each simulation is given in Table S2.

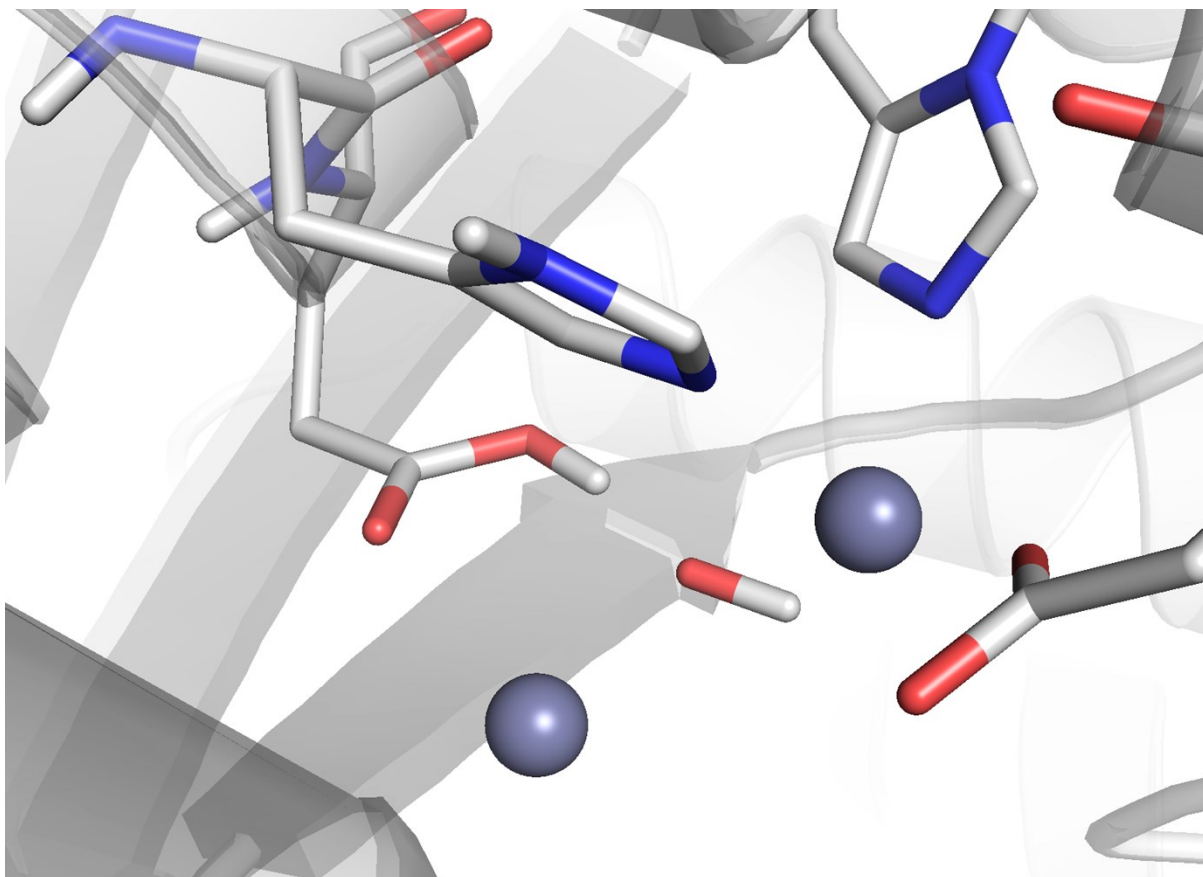
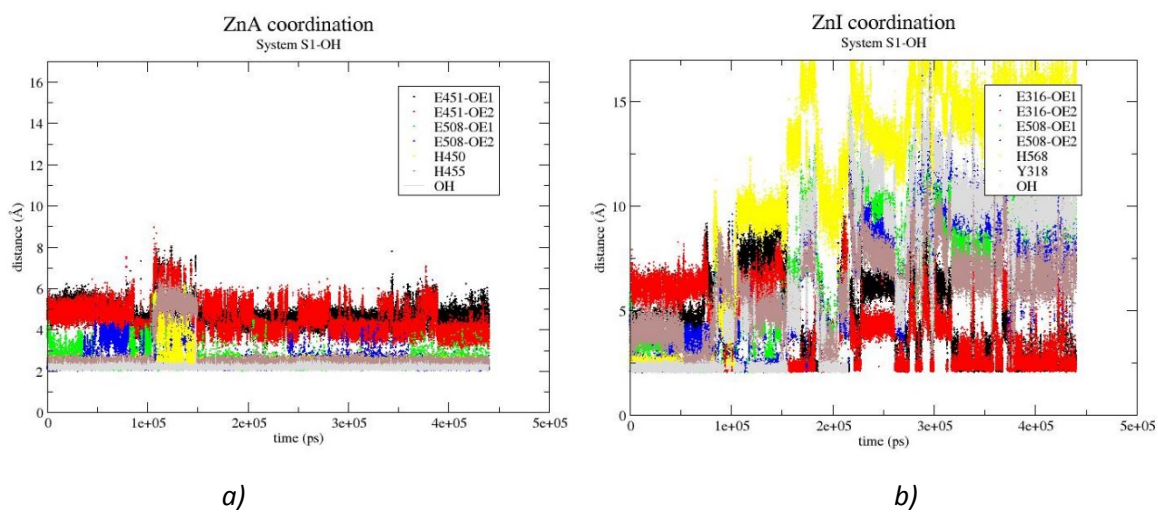


Figure S5. S1-OH⁻ structure obtained after 700 ns of MD simulation. ZnA is coordinated with H450, H455, E508 and OH⁻, and ZnI is coordinated with E451 and OH⁻.



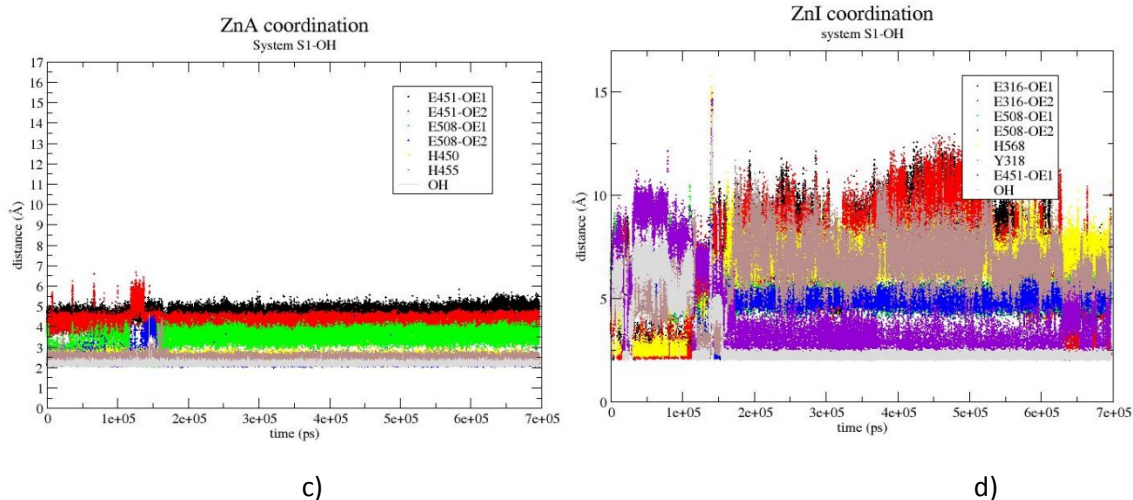


Figure S6. Coordination of zinc ions during 440 ns (a and b) and 700 ns (c and d) of MD simulations of S1-OH*(see Table S2) with 6-12 model 3 and ff03 and ff14SB force fields, respectively: a) and c) distances from ZnA; b) and d) distances from ZnI.

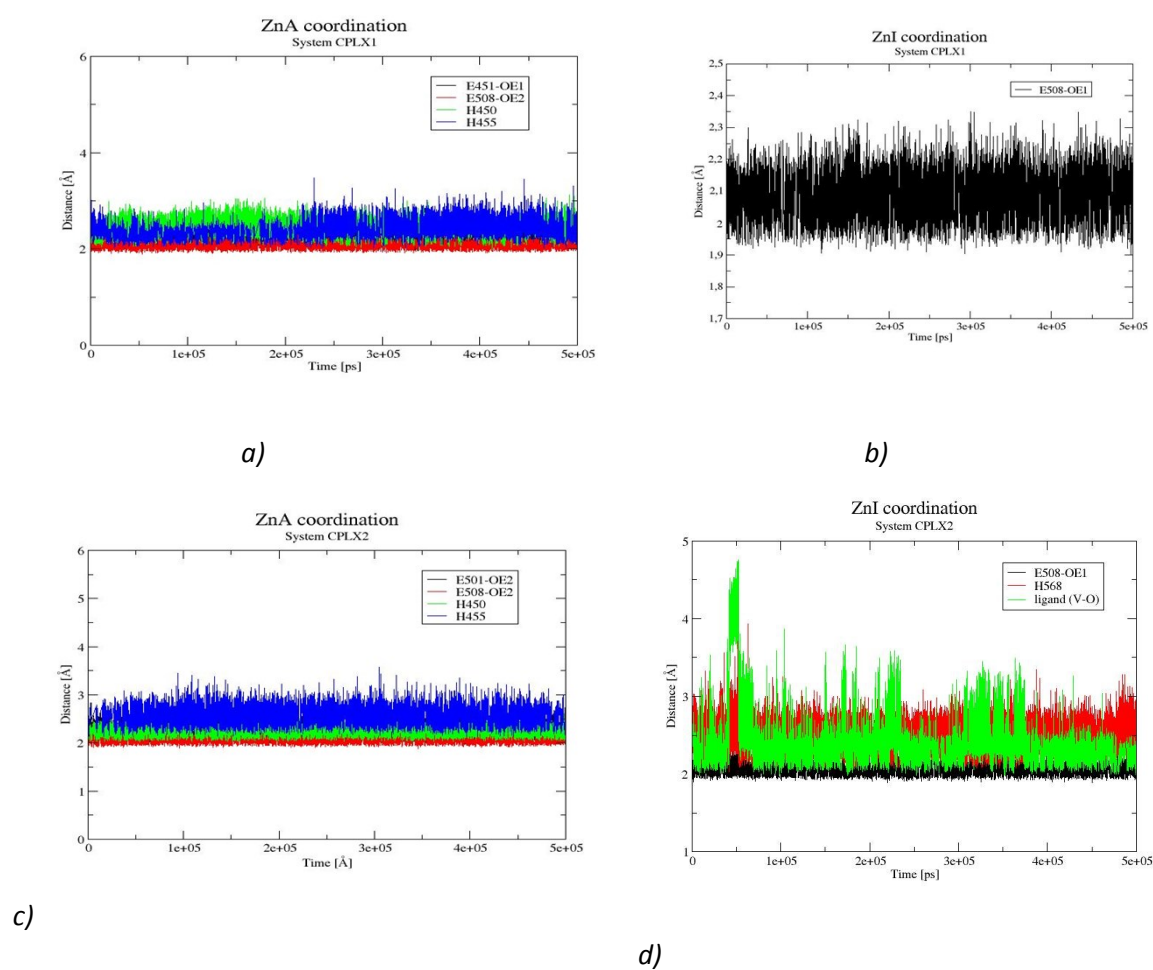


Figure S7. Coordination of zinc ions during 500 ns of MD simulations of **CPLX1** (a and b) and **CPLX2** (c and d) with model **D2**, see Table S2.

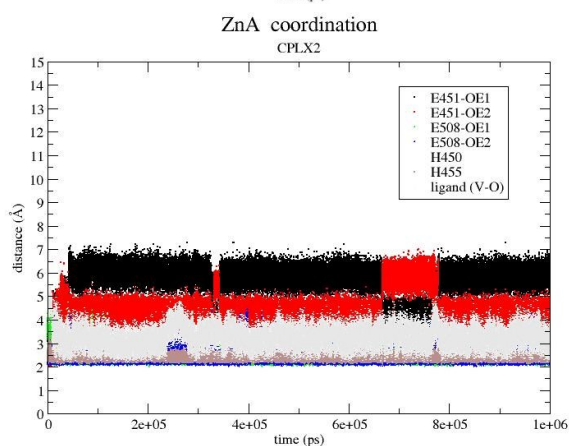
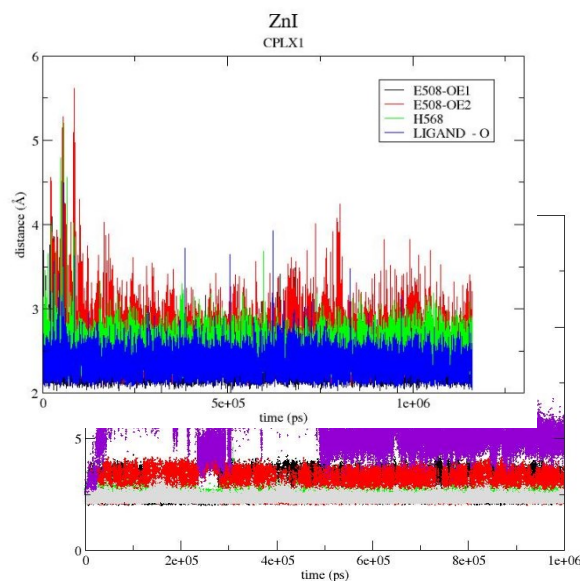
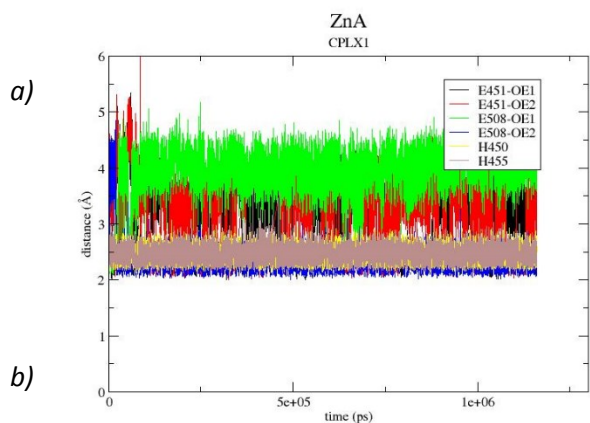
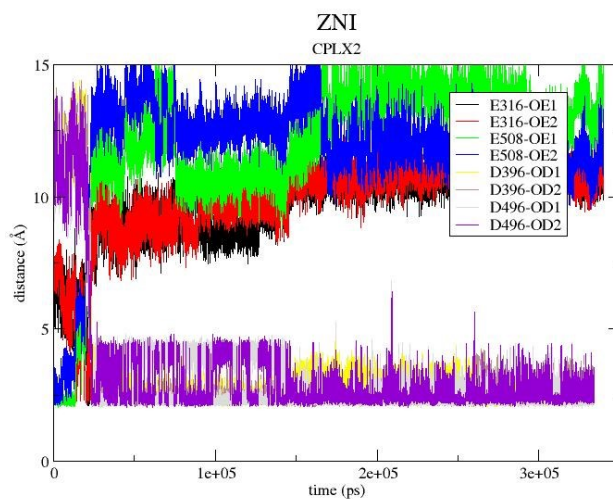
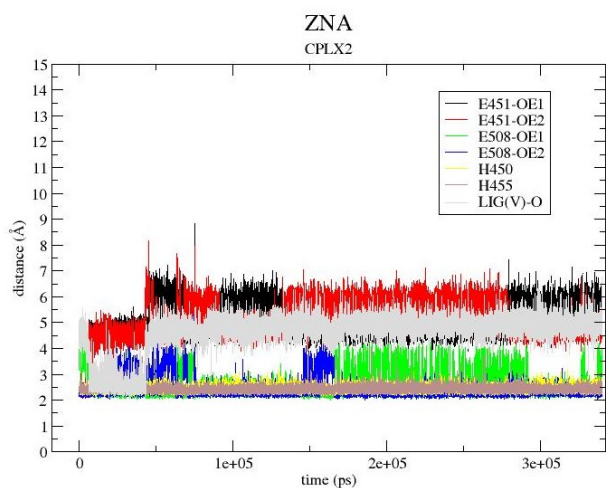
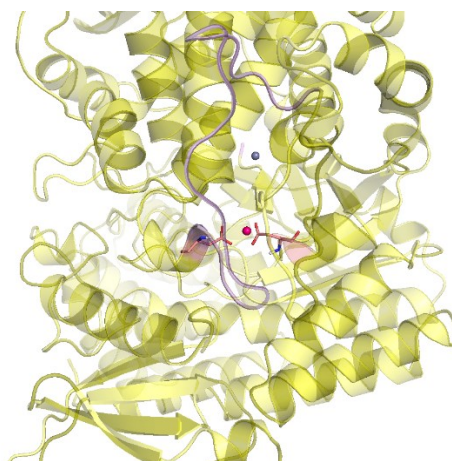


Figure S8. Coordination of zinc ions during 1.2 μ s of MD simulations of **CPLX1** with model **3** (a and b) and 1.0 μ s of MD simulations of **CPLX2** with model **3'** (c and d), see Table S2.





c)

Figure S9. Coordination of zinc ions during 340 ns of MD simulations of **CPLX2** with model **3** (a and b), c) structure at the end of 340 ns of MD simulation. Protein is shown as ribbon, zinc ions as spheres (ZnA gray, and ZnI magenta) and amino acids E396 and E496 coordinating ZnI are shown as sticks.

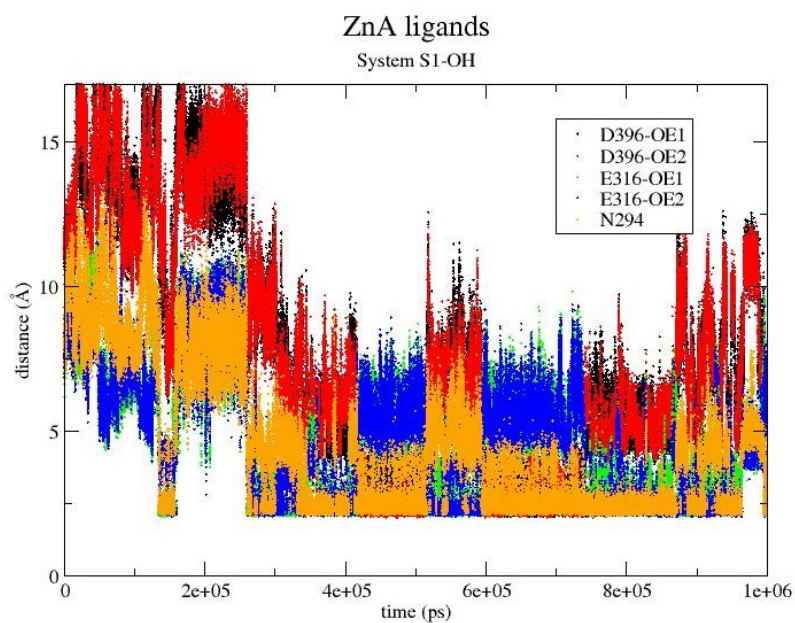
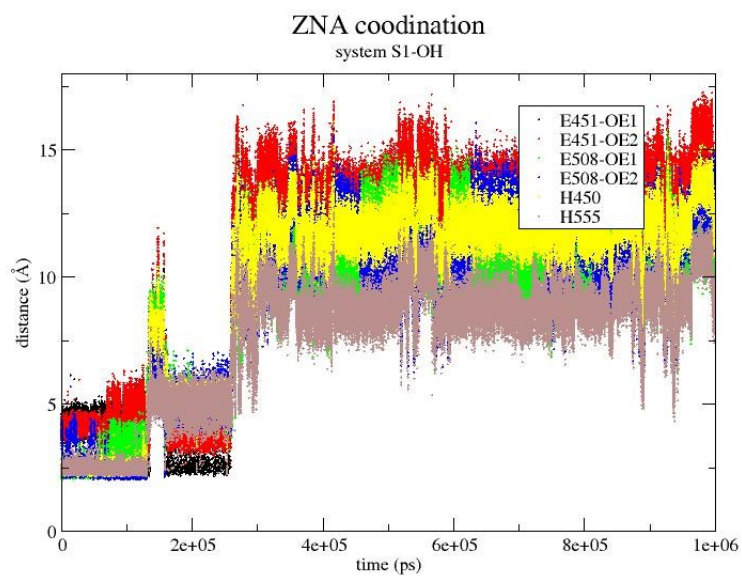


Figure S10. Exchange of the ZnA and ZnI positions during 1.0 μ s of MD simulations of S1-OH with model 3.

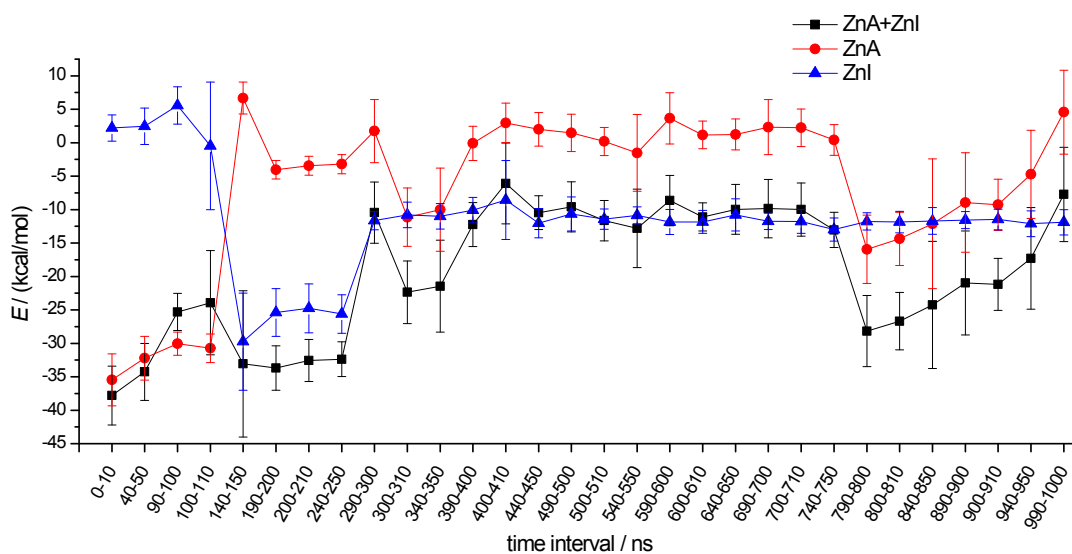


Figure S11. MMGBSA energies for ZnA and ZnI binding calculated at 10 ns intervals separated by 40 ns intervals throughout of 1.0 μ s long of MD simulations of **S1-OH** with model **3**.

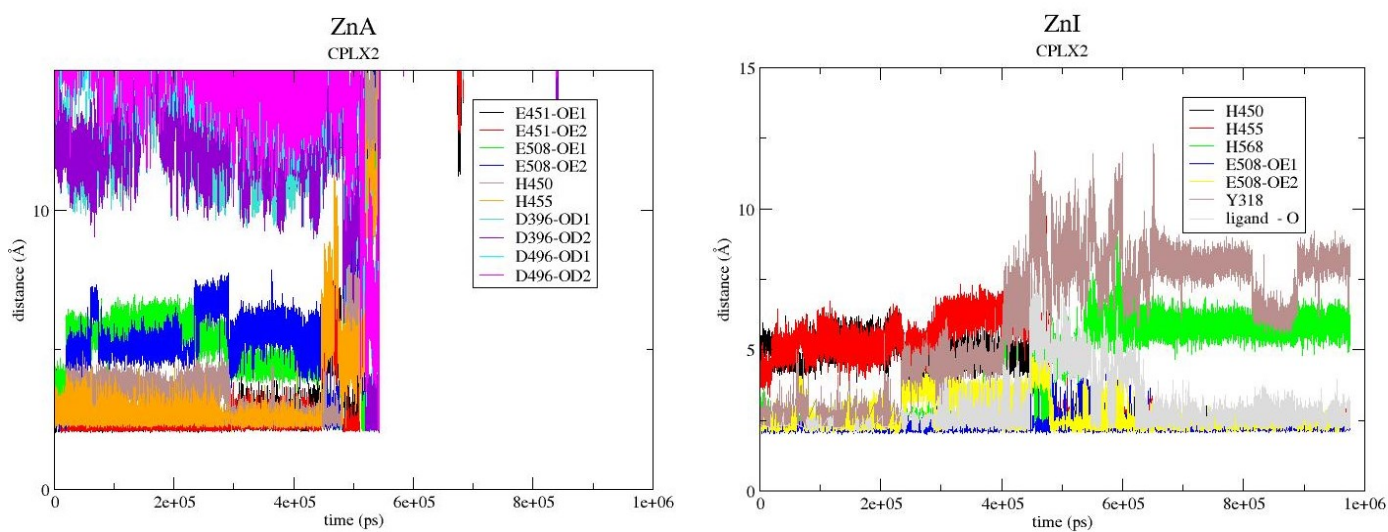


Figure S12. Exchange of the ZnA and ZnI positions and exit of ZnA from the protein traced during 980 ns of MD simulations of **CPLX2** with model **3r**.

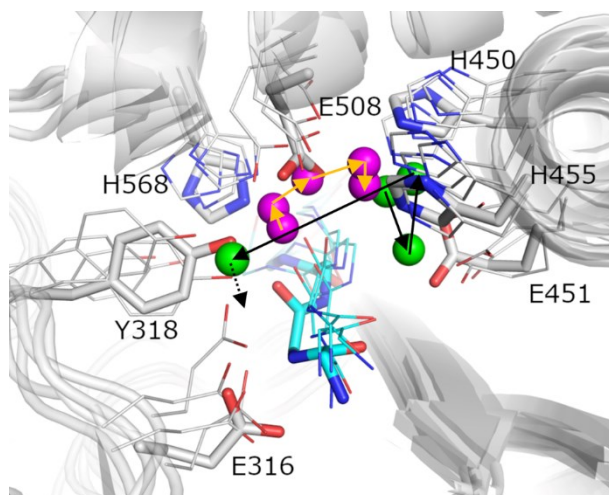


Figure S13. Exchange of the ZnA (green sphere) and ZnI (magenta sphere) positions and exit (indicated by dashed arrow) of ZnA from the protein traced during 720 ns of MD simulations of **CPLX2** with model **3r**. Amino acid residues (carbon atoms coloured grey, only side chains are shown) participating in metal ions coordination and peptide (carbon atoms coloured cyan, only main chain atoms are shown) are shown as sticks (initial positions are indicated with thicker sticks). Hydrogens are not shown.

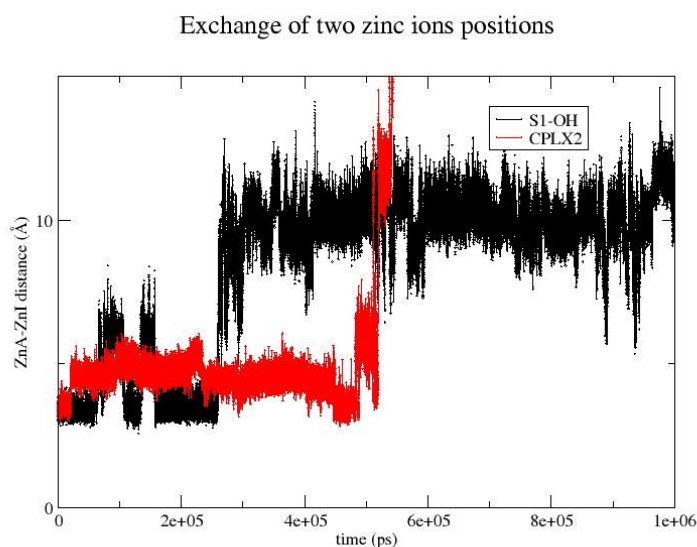


Figure S14. Distance between zinc ions during MD simulations of ligand-free hDPP III and its complex with peptide (IVYPW), in which the zinc ion moves from the inhibitory binding site to the active binding site and the zinc ion originally present in the active site moves away. Simulations were performed using 6-12 models **3** and **3r**, respectively. These simulations are indicated in Table S2 with superscript 'exe'.

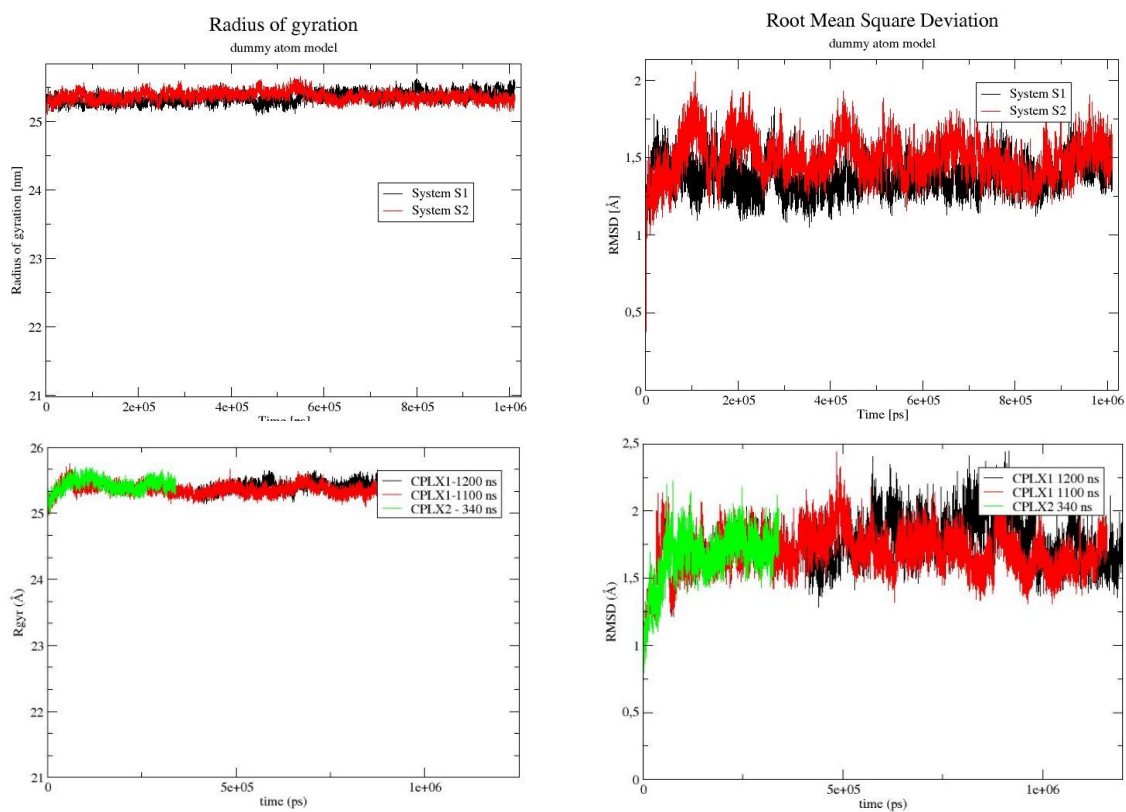
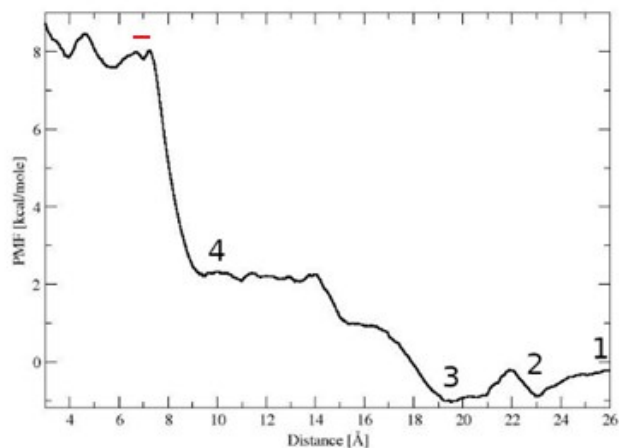
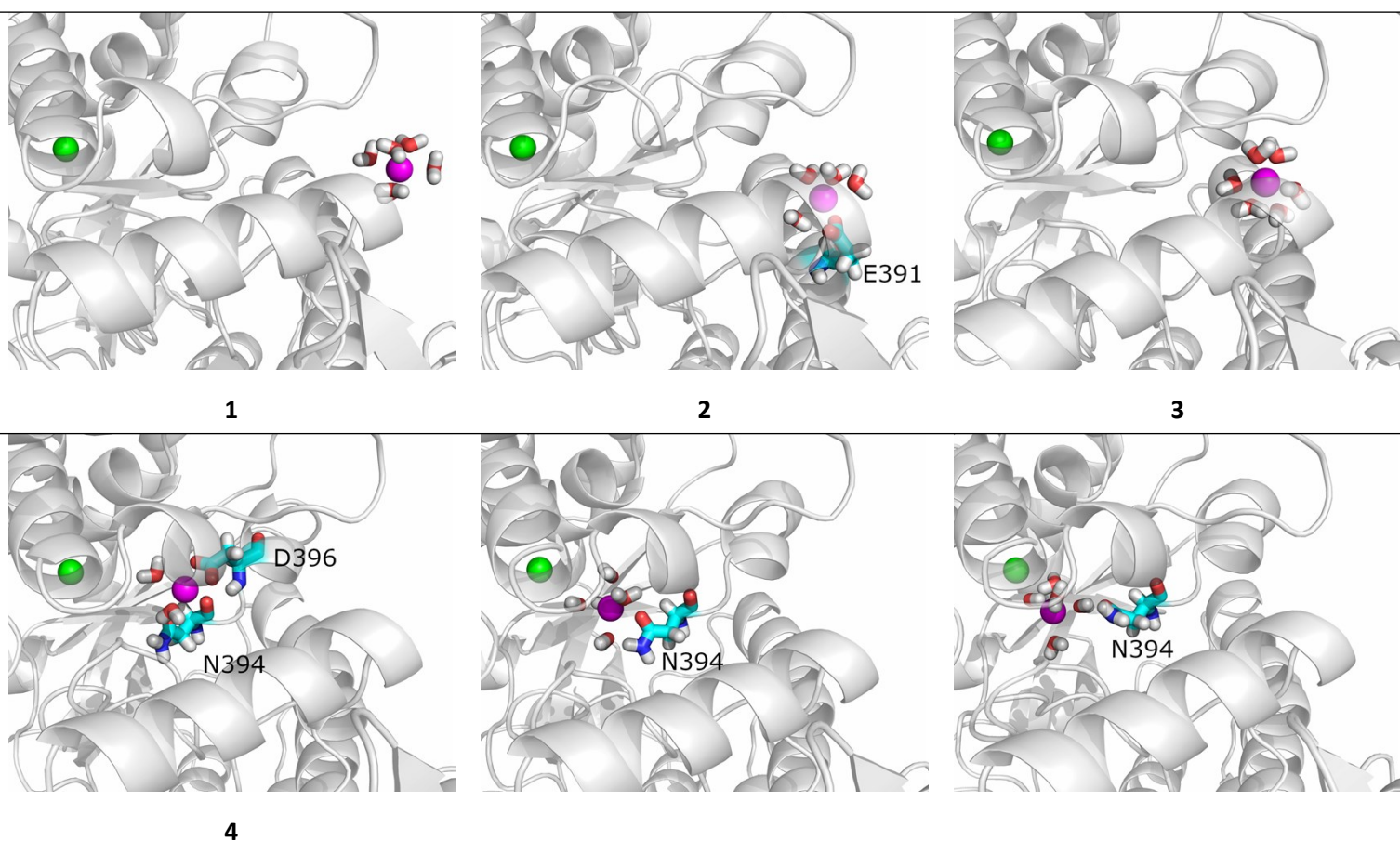


Figure S15. Radius of gyration (Rgyr) and root mean square deviation (RMSD) obtained during the most representative (and the longest) MD simulations using dummy atom and 6-12 models for metal ions.

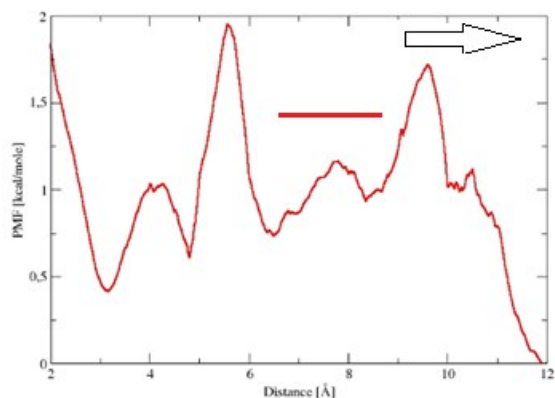


(A)

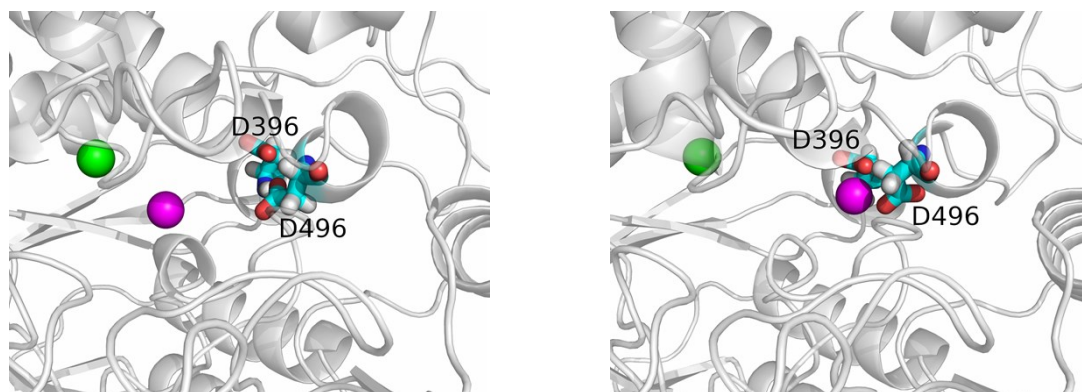


(B)

Figure S16. Free energy barriers for translocation of zinc ions (ZnI) from bulky water to the interior of hDPP III, near the position of the catalytically active zinc ion (ZnA). (A) Potential of the mean force profile. Numbers (1-3) in the plot indicate the initial position and the positions of the minima shown in the figure below. Number 4 indicates the structures representing the zinc ion trapped by D396 as it enters the interior of the protein. (B) Shown are the structures indicated in the plot and the two structures representing the entry of the zinc ion into the cleft (from the region indicated by the red line above), with D496 serving as the metal ion transporter. ZnI is shown as a magenta sphere, ZnA as a green sphere.



(A)



(B)

Figure S17. Free energy barriers to translocation of the zinc ion from the inhibitory binding site to the protein surface. (A) Potential of the mean force profile. The arrow indicates the direction of the force. (B) Left - structure from the region indicated by the red line above, and right - final structure. ZnI is shown as a magenta sphere, and ZnA as a green sphere. The position of ZnI in the final structure is very similar to its position in the structure shown in Fig. S9. c, which was obtained during 340 ns of the MD simulations of **CPLX2**, when ZnI spontaneously moved towards the entrance of the interdomain gap.

REFERENCES:

- 1 W. D. Cornell, P. Cieplak, C. I. Bayly, I. R. Gould, K. M. Merz, D. M. Ferguson, D. C. Spellmeyer, T. Fox, J. W. Caldwell and P. A. Kollman, A second generation force field for the simulation of proteins, nucleic acids, and organic molecules, *J. Am. Chem. Soc.*, 1995, **117**, 5179–5197.
- 2 C. Jarzynski, Nonequilibrium Equality for Free Energy Differences, *Phys. Rev. Lett.*, 1997, **78**, 2690–2693.

